J Mater Sci (2007) 42:5778–5784
DOI 10.1007/s10853-006-1194-1

Chromium vaporization of the ferritic steel Crofer22APU and ODS $Cr5Fe1Y_2O_3$ alloy

E. Konysheva · U. Seeling · A. Besmehn · L. Singheiser · K. Hilpert

Received: 3 December 2005 / Accepted: 27 January 2006 / Published online: 25 April 2007

Abstract The chromium vaporization rate of the Crofer22APU steel as compared to $Cr5Fe1Y_2O_3$ alloy was studied under humidified air at 800 °C over a period of up to 1300 h by using the transpiration method. Under oxidizing atmosphere, the Crofer22APU steel forms a $(Cr,Mn)_3O_4$ spinel layer on the surface, which hinders chromium release at 800 °C by about a factor of 3 as compared to $Cr5Fe1Y_2O_3$ alloy forming a pure chromia scale. The impact of minor alloying additives in the Crofer22APU ferritic steel on the chromium vaporization was considered. The steel with the lowest amount of Al and Si in the matrix exhibits a low chromium vaporization rate over 1300 h. The microstructure and composition of the oxide scales and surfaces formed were investigated using high-resolution scanning electron microscopy, X-ray photoelectron spectroscopy and time-of-flight secondary ion mass spectrometry. The results obtained give insight into the chromium vaporization mechanism.

E. Konysheva · L. Singheiser · K. Hilpert
Institute for Materials and Processes in Energy Systems (IWV-2), Research Centre Juelich, 52425 Juelich, Germany

Present Address:
E. Konysheva (✉)
School of Chemistry, Purdie Building, University of St Andrews, St Andrews, Fife, KY 16 9ST, UK
e-mail: ek31@st-andrews.ac.uk

U. Seeling · A. Besmehn
Central Division of Analytical Chemistry (ZCH), Research Centre Juelich, 52425 Juelich, Germany

Introduction

Ferritic stainless steels are now widely used as interconnect materials in solid oxide fuel cells (SOFC) operated at medium temperatures [1]. Crofer22APU ferritic steel developed by Research Centre Juelich (Germany) and commercialized by ThyssenKrupp VDM (Germany) is one of the most promising materials. The majority of papers published on the Crofer22APU ferritic steel [1–8] have focused on the oxidation/corrosion behavior of this steel in cathode-and /or anode-side gases, conductivity of the thermally grown scale, effect of the thickness of the steel on lifetime limit and thermal expansion behaviour. The oxide scale formed on the surface of the Crofer22APU ferritic steel was described in the literature as a duplex structure made of an outer Cr, Mn spinel layer and an inner Cr_2O_3 layer, thereby increasing the electrical conductivity of the scale and improving the interface stability as compared to traditional chromia-forming alloys [1, 2, 4, 9, 10]. However, chromium release of Cr-containing materials is usually observed under an oxidizing atmosphere due to the formation of gaseous high-valent chromium oxide and oxyhydroxide species, in particular $CrO_3(g)$ and $CrO_2(OH)_2(g)$ [11]. In the case of an SOFC system, these gaseous species are electrochemically reduced in porous perovskite cathode, inhibiting the oxygen reduction necessary for the operation of the SOFC [11, 12]. Therefore, a study of the chromium vaporization of steels and an understanding of the mechanism of this interface process is of significance for increasing service life and the production of cost-effective SOFC systems.

The objectives of the present work are to systematically investigate the chromium vaporization of the Crofer22APU ferritic steel as compared to the oxide-dispersion-strengthened (ODS) chromium-base alloy Ducrolloy

$Cr5Fe1Y_2O_3$ as the source of the degradation of an SOFC system and to study the effect of minor alloying additives in the steel matrix on the chromium vaporization rate.

Experimental

Materials investigated

The commercial ferritic Crofer22APU-1st and Crofer22APU-2nd steels supplied by Thyssen Krupp VDM, the semi-commercial JS-3 steel supplied by Thyssen Krupp KTN and the oxide-dispersion-strengthened (ODS) chromium-base alloy Ducrolloy $Cr5Fe1Y_2O_3$ supplied by Plansee were studied. The chemical composition of the materials is listed in Table 1. Planar alloy plates with dimensions of $80 \times 20 \times 4.1...1.8$ mm^3 were used for the vaporization experiments. The surface of the samples was ground using SiC paper of 1200 mesh and then cleaned with ethanol using an ultrasonic bath. All materials were pre-oxidized at a temperature of 800 °C for 100 h under static air in order to grow continuous oxide scale at the surface of alloys. These samples were further used for the transpiration experiments.

Transpiration method

The transpiration method was used to measure the chromium vaporization under a controlled humidified gas-flow rate [13]. This method allows the SOFC condition in the air flow channels to be simulated. A schematic representation of the apparatus is given in Fig. 1.

The quartz tube consists of the vaporization chamber and the condenser, which are connected by a ground joint. The sample is placed in the vaporization chamber and is separated by a quartz filter and a capillary in order to minimize outdiffusion of gaseous species. In addition, the temperature of the isothermal zone along the sample is monitored by 3 Chromel—Alumel (type K) thermocouples. The quartz tube is heated up to the measurement temperature at a rate of 18 °C/min. The flow of a carrier gas is started after the furnace has reached the measurement temperature. The flow of the carrier gas (in this study air) is determined by a flow meter (Type 5850TR, Brooks, The Netherlands). The water partial pressure is adjusted by the temperature of a cooler coupled to the humidifier and checked with an *r*H-meter (Type Hygroclip SC05, Rotronic, Switzerland).

In the heated vaporization chamber of the quartz tube, volatile chromium species vaporize from the sample surface. A stream of carrier gas transports the volatile species from the vaporization chamber downstream to the condenser, which is cooled to room temperature. The vaporizing species condense in the condenser of the quartz tube. After completion of the measurement, the carrier gas flow is stopped and the furnace cooled down to room temperature (RT) at a rate of 15 °C/min (from 800 to 500 °C) and then at an average rate of 2 °C /min (from 500 °C to RT).

After the measurements, the chromium condensed in the condenser of the quartz tube was dissolved by concentrated HCl acid (Suprapur®, Merck KGaA, Germany). The chromium concentration in the solutions is determined by inductively coupled plasma-quadrupole mass spectrometry (ICP-QMS) [14]. The instrument used is a SCIEX Elan 6000 (Perkin Elmer, USA).

The experiments with different samples were carried out at a temperature of 800 °C over a period of up to 1300 h under non-equilibrium conditions using air with a humidity of 60 % at 25 °C corresponding to$P_{H_2O} = 2 \cdot 10^3$ Pa and gas flow rates of 1.3 and 2.4 L_n/min (''n'' stands for ''under normal conditions'', i.e., $T_0 = 273.15$ K, $P_0 = 1$ atm). Each transpiration measurement was carried out two or three times in order to check the reproducibility.

Surface and interface characterization

The microstructure of the oxide scales and the interfaces formed was analyzed by scanning electron microscopy (SEM). The SEM investigation was carried out with a LEO 1530 (Zeiss, Germany) scanning electron microscope equipped with an energy dispersive X-ray (EDX) spectrometer of the Inca 400 type (Oxford Instruments, UK).

Time-of-flight secondary ion mass spectrometry (TOF-SIMS) and X-ray photoelectron spectroscopy (XPS) were used to characterize the distribution of elements in the oxide scale formed and also the chemical composition of the surface. TOF-SIMS was carried out with a TOF-SIMS IV mass spectrometer (ION-ToF GmbH, Germany) using a

Table 1 Chemical composition of materials investigated (wt. %)

	Fe	Cr	Mn	Al	Si	Ni	Ti	La	Others
$Cr5Fe1Y_2O_3$	5.4	93.7	0.006	<0.01	<0.005	≤ 0.005	—	—	0.49 Y, 0.42 O
Crofer22APU-1st	Bal.	23	0.41	0.12	0.1	0.16	0.05	0.08	Cu, V, Co, Nb, Ta, Zr
Crofer22APU-2nd	Bal.	22.2	0.46	0.02	0.02	0.16	0.05	0.07	
JS-3	Bal.	23	0.40	<0.01	<0.01	<0.002	0.05	0.09	

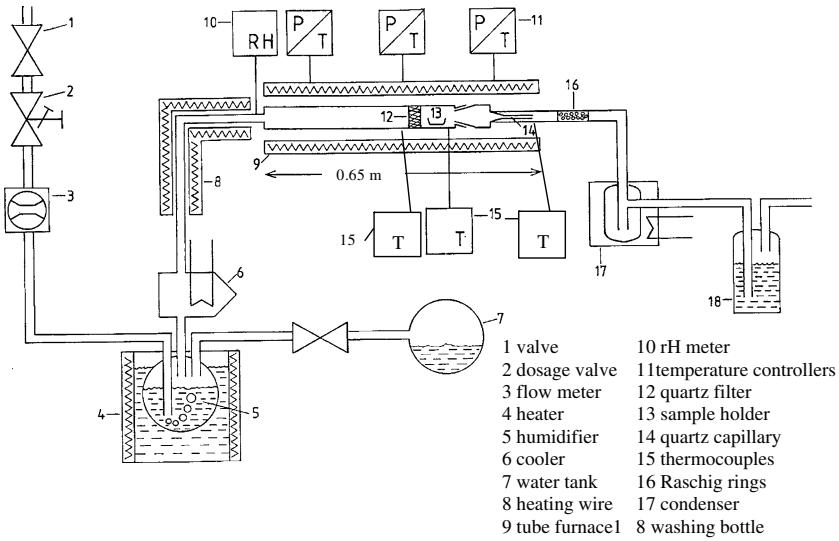

Fig. 1 Experimental setup used for the transpiration measurements [10, 12]

15 keV Ga^+ ion beam for analysis (raster size 15.6 × 15.6 μm^2). For XPS characterization, Cr $2p_{3/2}$, $Mn2p_{3/2}$, Fe $2p_{3/2}$ and O 1s, N 1s and C 1s core level spectra were recorded with an XPS 5600 spectrometer (Physical Electronic, USA) using monochromatic AlK_α radiation (hν = 1486.4 eV) at an analyzer pass energy of 11.75 eV. The X-ray spot was about 2 × 5 mm^2, and the analyzing aperture was about of 800 μm in diameter.

Results

Experimental results on the chromium vaporization of alloys supplemented by the characterization of the microstructure of the interfaces and the surfaces formed are presented in Figs. 2–4 and Table 2. Figure 2 represents the same experimental data on chromium vaporization in two different ways. The chromium vaporization rate of the alloys investigated, which means the amount of chromium vaporized per sample surface area unit and per time unit, is shown in Fig. 2a. The kinetics of the total amount of chromium vaporized per sample surface area is presented in Fig. 2b. First, the results on the chromium vaporization of $Cr5Fe1Y_2O_3$ alloy, which was chosen as a reference material, will be reported, and then the data for the Crofer22APU steel will be presented as compared to those for $Cr5Fe1Y_2O_3$ alloy.

$Cr5Fe1Y_2O_3$ alloy

Chromium vaporization of $Cr5Fe1Y_2O_3$ alloy

Chromium transport is markedly dependent on the rate of air flow passed over the specimens [15]. Under non-equilibrium conditions, each vaporizing chromium species is immediately transported downstream into the condenser and the chromium transport rate measured by the transpiration method equals the chromium vaporization rate. Figure 2 illustrates the time dependence of the chromium vaporization of $Cr5Fe1Y_2O_3$ alloy under two different gas flow rates. It can be seen that the chromium vaporization rate of $Cr5Fe1Y_2O_3$ alloy under gas flow rates of 1.3 and

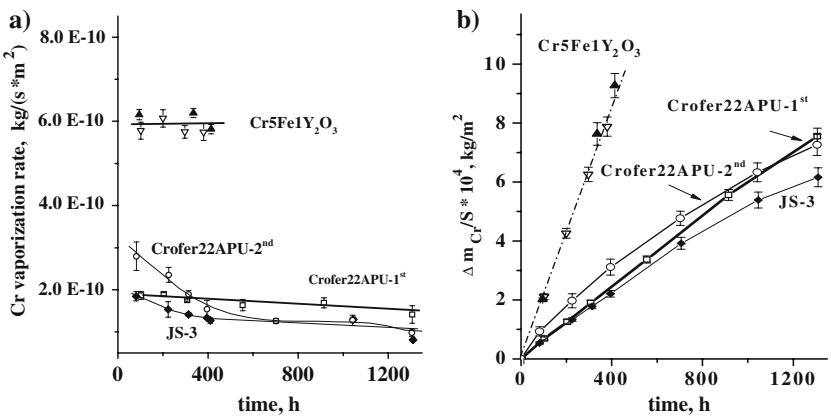

Fig. 2 Time dependence of the chromium vaporization rate (**a**) and kinetics of the chromium vaporization (**b**) of the Crofer22APU-1st (□), Crofer22APU-2nd (○), JS-3 (♦) steels and alloy $Cr5Fe1Y_2O_3$ (1.3 L_n/min, (▽), and 2.4 L_n/min, (▲)) at 800 °C under humidified air ($P_{H_2O} = 2 \cdot 10^3$ Pa)

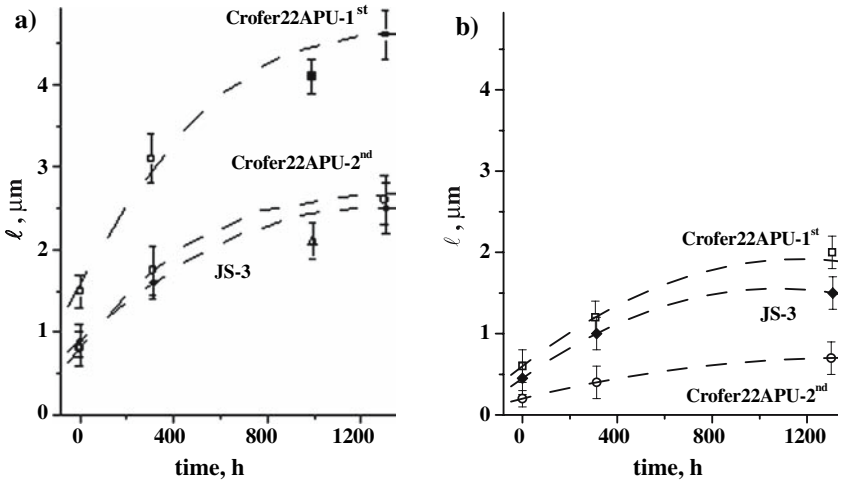

Fig. 3 The growth of the oxide scale (**a**) and of the $(Cr,Mn)_3O_4$ spinel constituent in the oxide scale (**b**) on the steels during exposure at 800 °C to humidified air ($P_{H_2O} = 2{\cdot}10^3$ Pa, gas flow rate of 1.3 l_n/min). Steels: Crofer22APU-1st (□), Crofer22APU-2nd (○), JS-3 (♦). For comparison the data from Ref. [3] are shown: Crofer22APU-1st (■), JS-3 (Δ) (the oxide scale grew under static air)

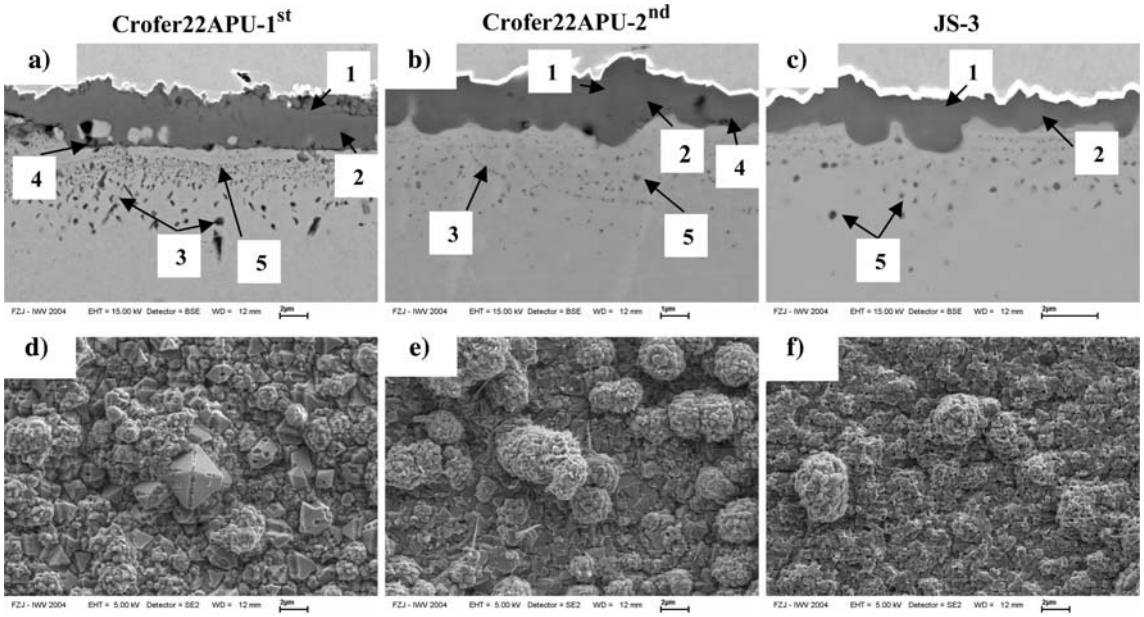

Fig. 4 SEM images of the cross-section (**a**–**c**) and of the surface (**d**–**f**) of the Crofer22APU-1st, Crofer22APU-2nd and JS-3 steels after the transpiration experiments at 800 °C for 300 h under humidified air ($P_{H_2O} = 2{\cdot}10^3$ Pa, gas flow rate of 1.3 L_n/min). 1—$(Mn,Cr)_3O_4$; 2—Cr_2O_3; 3—Al_2O_3 ; 4—SiO_x; 5—TiO_x

2.4 L_n/min is nearly the same, Fig. 2a, and shows linear kinetics over the period investigated, Fig. 2b. This is in a good agreement with the previous result. It was reported in [16] that the chromium vaporization of pure chromia in oxygen exhibits linear time dependence and is limited by surface kinetics.

Microstructure and surface characterization of the oxide scale formed

EDX analysis revealed a formation of continuous Cr_2O_3 scale as thick as 0.5 μm on the surface of $Cr5Fe1Y_2O_3$ alloy after preoxidation under static air at a temperature of 800 °C for 100 h. As was shown by XPS and TOF-SIMS, the surface layer of the oxide scale formed contains traces of iron and yttrium distributed in a random way. Moreover, large precipitates of yttrium were found in the sub-scale zone of the alloy. After the transpiration experiment over 300 h under different air flow rates, the Cr_2O_3 oxide scale grew to about 1 μm. According to TOF-SIMS, the concentration of iron in the surface layer of the oxide scale increases, whereas that of yttrium decreases slightly. The large precipitates of yttrium disappeared and only traces of this element uniformly distributed within the sub-scale zone of this alloy can be observed.

Table 2 XPS analysis of the steel surface before and after the transpiration experiments at 800 °C (data evaluated from the overview spectrum)

Steels	[Mn]/[Cr] ratio	
	Preoxidized under static air, 100 h	Gas flow rate 1.3 L_n/min,P_{H_2O} = $2 \cdot 10^3$ Pa, 1300 h
Crofer22APU-1st	1.19 ± 0.09[a]	1.37 ± 0.10
Crofer22APU-2nd	0.93 ± 0.07	1.43 ± 0.10
JS-3	1.05 ± 0.08	1.39 ± 0.10

[a] Error bars refer to 1 standard deviation

Crofer22APU steel

Chromium vaporization of Crofer22APU steel

The region where the chromium transport rate of the Crofer22APU steel is independent of the gas-flow rate was determined by special measurements [17] and found to be higher than 1.2 L_n / min. Cr vaporization of the Crofer22APU-1st, Crofer22APU-2nd and JS-3 steels is presented in Fig. 2a, b. The chromium release of the Crofer22APU-1st is lower by about a factor of 3 as compared to that of Cr5Fe1Y_2O_3 alloy, Fig. 2a.

The Crofer22APU-1st, Crofer22APU-2nd and JS-3 steels have nearly the same general composition, but the content of minor alloying additives (for instance, Al, Si and others, cf. Table 1) was varied in order to find the factors which influence the chromium vaporization of the steels forming an outer $(Cr,Mn)_3O_4$ spinel layer. Some discrepancies in the chromium vaporization rate of these steels are clearly observed, Fig. 2a. For instance, the JS-3 steel shows the lowest chromium release of these three materials over the 1300 h of the transpiration measurements, Fig. 2a. The chromium vaporization rate of the Crofer22APU-2nd steel is higher as compared to those of the Crofer22APU-1st and JS-3 steels after 100 h, Fig. 2a, and gradually decreases during the following exposure to humidified air. The chromium vaporization rate of the Crofer22APU-2nd and JS-3 steels is comparable after 600 h. The chromium release of the Crofer22APU-1st steel is practically independent of time, Fig. 2a, and shows near-linear kinetics like Cr5Fe1Y_2O_3 alloy, Fig. 2b. However, the JS-3 and Crofer22APU-2nd steels display some deviations from linearity.

In summary, the following tendencies for the change of the chromium vaporization rate of the steels investigated can be expressed for different time periods

$$\text{before } 400\,\text{h} \quad \text{JS - 3} \leq \text{Crofer22APU - 1st} < \text{Crofer22APU - 2nd} \tag{1}$$

$$\text{after } 400\,\text{h} \quad \text{JS - 3} \approx \text{Crofer22APU - 2nd} < \text{Crofer22APU - 1st.} \tag{2}$$

Microstructure and surface characterizations of the oxide scale formed

The total thickness of the oxide scale formed on the surface of the Crofer22APU-1st, Crofer22APU-2nd and JS-3 steels preoxidized under static air at a temperature of 800 °C for 100 h amounts to about 1.5, 0.8 and 0.9 μm, respectively, Fig. 3a. The following tendency can be established for oxide scale growth over the investigated period

$$\text{JS - 3} \approx \text{Crofer22APU - 2nd} < \text{Crofer22APU - 1st.} \tag{3}$$

The growth of the oxide scale obeys a near-parabolic law, which is in good agreement with the previous results [1, 3, 4]. In all cases, the oxide scale mainly consists of an outer $(Cr,Mn)_3O_4$ spinel layer and an inner Cr_2O_3 layer. A difference in the thickness of a $(Cr,Mn)_3O_4$ spinel constituent in the scale was found, Fig. 3b, and the following tendency (4),

$$\text{Crofer22APU - 2nd} < \text{JS - 3} < \text{Crofer22APU - 1st.} \tag{4}$$

In addition, different types of internal oxidation were observed for these steels, Fig. 4a–c. Alumina, SiO_x and TiO_x precipitates were formed in the area of internal oxidation of the Crofer22APU-1st and Crofer22APU-2nd steels, whereas TiO_x precipitates were only revealed in that of the JS-3 steel.

SEM images of the surface of the Crofer22APU-1st, Crofer22APU-2nd and JS-3 steels after 300 h of transpiration experiments are presented in Fig. 4d–f. The surface of the JS-3 steel is the most homogeneous as compared to those of the Crofer22APU-2nd and Crofer22APU-1st steels. Cr, Mn, Fe, Ti and O elements are uniformly distributed over the surface, as was shown by SEM/EDX and TOF-SIMS. This semi-commercial steel shows relatively low chromium vaporization over the whole time period (Fig. 2a, Section ''Chromium vaporization of Crofer 22APU steel''). Needle-shaped crystals of iron oxide, crystals of titanium oxide and associates as large as about 4 μm mainly consisting of small $(Cr,Mn)_3O_4$ spinel crystals can be clearly observed on the surface of the Crofer22APU-2nd steel, Fig. 4e. In the case of the Crofer22APU-1st steel, the surface is strongly non-homoge-

neous, Fig. 4d. Very large crystals of $(Cr,Mn)_3O_4$ spinel with decayed edges were revealed in addition to TiO_x and MnO_x crystals. The following trend could be noted: the lower the content of Al and Si additives in the matrix of the steel, the more homogeneous surface is of the oxide scale formed.

According to XPS analysis, the [Mn]/[Cr] ratio on the surface of the preoxidized steel slightly increases in the following order, Table 2,

$$\text{Crofer22APU - 2nd} \rightarrow \text{JS - 3} \rightarrow \text{Crofer22APU - 1st.} \quad (5)$$

The chromium depletion on the surface of the spinel layer becomes a little larger in the course of the transpiration measurements, Table 2. In the case of Crofer22APU-1st, the chromium surface concentration only changed from 9.7 atom% to 7.5 atom% (after 300 h) and amounts to 7.7 atom% after 1300 h. The same [Mn]/[Cr] ratio, however, was found for all steels after 1300 h, Table 2, in spite of the difference observed in the thickness of the Cr,Mn spinel constituent, Fig. 3b and tendency (4).

Discussion

The chromium concentration on the surface of $Cr5Fe1Y_2O_3$ alloy and the Crofer22APU-1st steel preoxidized under static air amounts to about 40 and 10 atom%, respectively. The chromium release of $Cr5Fe1Y_2O_3$ alloy should therefore be higher by about a factor of 4 as compared to that of the Crofer22APU- 1st steel. The difference in the chromium vaporization of these materials measured by the transpiration methods shows a coefficient of 3, which agrees satisfactorily with the expected value. This could indicate that the chromium vaporization rate is proportional to the chromium surface concentration. It cannot, however, be ruled out that additional factors influence the chromium vaporization of steels forming duplex $(Cr,Mn)_3O_4/Cr_2O_3$ scale.

The chromium vaporization of the Crofer22APU-2nd and JS-3 steels shows some deviation from linearity unlike the Crofer22APU-1st steel and $Cr5Fe1Y_2O_3$ alloy. If the chromium vaporization of the steel forming an outer (Cr,Mn) spinel layer were controlled by oxygen diffusion through the oxide scale formed, then a correlation between the chromium vaporization rate and the total thickness of the oxide scale should be observed. In other words, a steel with the thickest oxide scale should show the lowest vaporization rate and the kinetics of the chromium vaporization process should obey a near-parabolic law. If the chromium diffusion through the $(Cr,Mn)_3O_4$ spinel layer were a limiting stage for the chromium vaporization process, then steels with the thickest and the thinnest spinel layer should show the lowest and the highest vaporization rate, respectively.

The $(Cr,Mn)_3O_4$ spinel constituent in the oxide scale formed on the surface of the Crofer22APU-2nd steel is the thinnest over the period investigated, Fig. 3b. This steel only shows relatively high chromium vaporization rate for a period of up to 400 h, tendency (1). Further, however, the chromium vaporization rate of this steel is comparable with that of the JS-3 steel, which exhibits the lowest vaporization rate over 1300 h. In contrast to this, the difference in the thickness of the spinel constituent grown on the surface of these steels amounts to about a factor of 2, Fig. 3b. The difference in the chromium vaporization of the JS-3 and Crofer22APU-2nd steels observed over the initial period could be related to the slower formation of the spinel layer on the surface of the Crofer22APU-2nd steel. The measured chromium vaporization rate seems to be a superposition of the chromium vaporization of chromia and of $(Cr,Mn)_3O_4$ spinel, if the thickness of the continuous spinel constituent in the scale is less than about 0.5 μm. The thickness of the spinel constituent in the oxide scale is of importance for an initial operation period and other factors control the chromium vaporization process after the $(Cr,Mn)_3O_4$ spinel layer has become as thick as about 0.5 μm.

The Crofer22APU-1st steel, which possesses the thickest oxide scale and $(Cr,Mn)_3O_4$ spinel constituent in the oxide scale, Fig. 3, does not show the lowest vaporization rate over the whole time period, Fig. 2a. For instance, the total thickness of the oxide scale and the thickness of the spinel constituent increased by about a factor of 3 after 1300 h, Fig. 3a,b. However, over the same time period the chromium vaporization rate changed from $1.9 \cdot 10^{-10}$ to $1.4 \cdot 10^{-10}$ kg/(s·m^2), Fig. 2a, and the chromium surface concentration only decreased by 2 atom%. The chromium vaporization of the Crofer22APU-1st steel shows a near-linear time dependence, Fig. 2b, and this interface process is most likely determined by the surface kinetics.

The following experimental fact is consistent with the above-mentioned assumption. The surface of the oxide scale formed on the Crofer22APU-1st steel is the most non-homogeneous as compared to those of the Crofer22APU-2nd and JS-3 steels. Well-shaped crystals of $(Cr,Mn)_3O_4$ spinel were observed on the surface of the Crofer22APU-1st steel preoxidized under static air at 800 °C for 100 h, while spinel crystals with destroyed kinks and edges were revealed after the transpiration measurements, Fig. 4d. Most probably, the formation of

heterogeneous complex molecules of the CrO_3 or $CrO_2(OH)_2$ types with a three-dimensional configuration preferably occurs on the kinks and edges of crystals or at the ''half-crystal position'', where the dimension limitation is less and binding energy differs from that in the volume [18, 19]. On the other hand, the vaporization rate of the homogeneous surface should be low due to the decrease in the number of active sites where the oxygen adsorption and the formation of complex molecules could occur. It seems that this is the reason for the observed low chromium vaporization rate of the JS-3 steel.

Conclusions

The chromium release of the Crofer22APU steel and of $Cr1Fe5Y_2O_3$ alloy was investigated. Formation of a $(Cr,Mn)_3O_4$ spinel layer as thick as half a micrometer on the surface of Crofer22APU decreases the chromium release by about a factor of 3 as compared to alloy forming a Cr_2O_3 scale. In this case, the chromium vaporization is most probably controlled by the surface kinetics.

Varying the minor additives in the Crofer22APU steel matrix influences the thickness of the oxide scale formed during exposure to humidified air, the $(Cr,Mn)_3O_4/Cr_2O_3$ ratio in the growing oxide scale as well as its morphology. This leads to some discrepancies observed in the chromium release of the Crofer22APU steel for different time periods. The kinetics of the chromium vaporization shows a deviation from linearity in the case of formation of a thin $(Cr,Mn)_3O_4$ spinel constituent in the oxide scale or the oxide scale with a homogeneous surface.

Acknowledgements The authors thank Dr. E. Wessel for the SEM analysis as well as Dr. U. Breuer and Ms. A. Scholl for the TOF-SIMS analysis.

References

1. Quadakkers WJ, Piron-Abellan J, Shemet V, Singheiser L (2003) Mater high temp 20(2):115
2. Piron-Abellan J, Shemet V, Tietz F, Singheiser L, Quadakkers WJ (2001) In: Yokokawa H, Singhal SC (eds) Proceedings of the 7th international symposium on solid oxide fuel cells (SOFC VII), Tsukuba, Japan, June 2001, The Electrochemical Society Proceedings, Pennington, NJ, 2001 PV. 2001–16, p 811
3. Huczkowski P, Christiansen N, Shemet V, Singheiser L, Quadakkers WJ (2004) In: Mogensen M (ed) Proceedings of the 6th European solid oxide fuel cell forum, Lucerne, Switzerland, July 2004, European Fuel Cell Forum, Oberrohrdorf, 2004 3:1594
4. Huczkowski P, Christiansen N, Shemet V, Piron-Abellan J, Singheiser L, Quadakkers WJ (2004) Mater Corr 55(11):825
5. Xie JJ, Yoo Y, Davidson I, Ghosh D (2004) In: Mogensen M (ed) Proceedings of the 6th European solid oxide fuel cell forum, Lucerne, Switzerland, July 2004, European Fuel Cell Forum, Oberrohrdorf, 2004 3:1602
6. Yang Z, Hardy JS, Walker MS, Xia G, Simner SP, Stevenson JW (2004a) J Electrochem Soc 151(11):A1825
7. Yang Z, Walker MS, Singh P, Stevenson JW, Norby T (2004b) J Electrochem Soc 151(12):B669
8. Yang Z, Xia G, Singh P, Stevenson JW (2005) Solid State Ionics 176:1495
9. Sakai N, Horita T, Xiong YP, Yamaji K, Kishimoto H, Brito ME, Yokokawa H, Maruyama T (2005) Solid State Ionics 176:681
10. Gindorf C, Singheiser L, Hilpert K (2001) Steel Res 72(11/12):528
11. Hilpert K, Das D, Miller M, Peck DH, Weiss R (1996) J Electrochem Soc 143:3642
12. Konycheva E, Penkalla H, Wessel E, Seeling U, Singheiser L, Hilpert K (2001) In: Singhal SC, Mizusaki J (eds) Proceedings of the 9th international symposium on solid oxide fuel cells (SOFC IX), Quebec, Canada, May 2005, The Electrochemical Society Proceedings, Pennington, NJ, 2001, PV 2005–07, p 1874
13. Merten U, Bell WE (1967) The characterization of high-temperature vapors. John Wiley and Sons, New York, London, Sydney, 1967, p 98
14. Becker JS (2002) Spectrochimica Acta B 57:1805
15. Kofstad P (1988) High temperature corrosion. Elsevier Applied Science Publishers Ltd, London and New York p 558
16. Hagel WS (1963) Trans ASM 56:583
17. Konysheva E, Penkalla H, Wessel E, Mertens J, Seeling U, Singheiser L, Hilpert K (2006) J Electrochem Soc 153:A765
18. Knacke O, Stranski IN (1956) Prog Metal Phys 6:181
19. Somorjai GA, Lester JE (1967) Prog Solid State Chem 4:1